UNIVERSITY OF MIAMI
ROSENSTIEL SCHOOL of MARINE & ATMOSPHERIC SCIENCE

Petrographic Characterization of Deep Water Ooids on the Florida Shelf

James Lachterman, Donald McNeill (advisor)

University of Miami, jel162@Miami.edu

Introduction

- Formation of ooid sands is generally thought to be a process that operates at relatively shallow (water) depth through tidal processes. [11, 12, 13, 14]
- Extensive formation during lowstands of sea level are not widely documented. [9, 16, 18]
- Deeper shelf ooids beds are generally rare. Drowned ooid samples have been previously sampled off the Florida coast. [18]
- Carbonates diagenesis can be linked to microbial activity. The level and rate of micritization and alteration observed in the ooid can potentially give insight into the site (depth) of diagenesis. [3, 4, 17, 20]
- This study examines ooid grains formed during the last glaciation and found at a depth on the shelf below the generally accepted level of the last sea-level lowstand (~120 m). [7]
- As such, our working hypothesis is that ooids can form by relatively strong currents during sea level lowstands. These formation environments are generally much less common (at least today) than tidal environments.

Methods

- Ooid sediment samples were collected from a series of cores part of an unrelated study from the east Florida shelf (Figure 1)
- Core 20 was chosen for analysis recovery of several meters of oolitic sand and mud. (Figure 2)
- Oolitic grains were collected in sample sizes of 200 grains per carbon stub. (Figure 3)
- Philips XL-30 environmental scanning electron microscope (SEM)

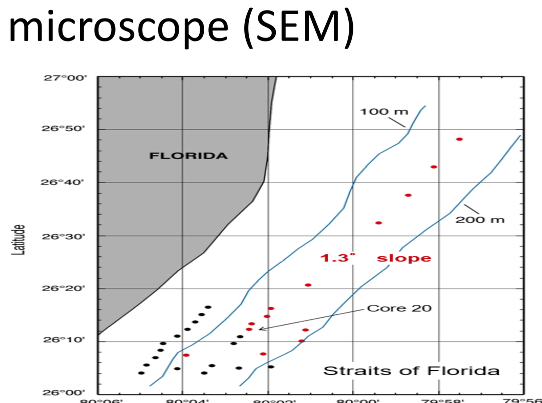

Figure 1: Generalized chart of core locations of the area of Fort Lauderdale, Florida. Depth markers alongside the blue lines (100 and 200 m contours) indicate depth of the Florida Shelf.

Figure 2: Ooid grainstone within a section (~230 cm) of Core 20. Ooid grainstone contains shell fragments and some very minor light-green mud.

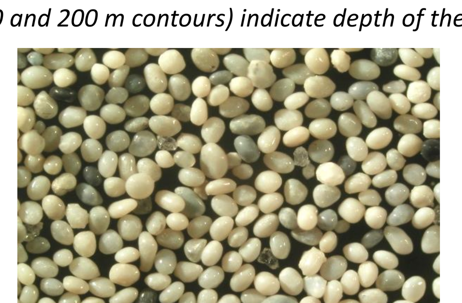

Figure 3: Photograph of washed ooid sand under a binocular microscope. Note the polished, and relatively well sorted ooid sand grains. Most ooids are about 250 microns in long diameter.

Results

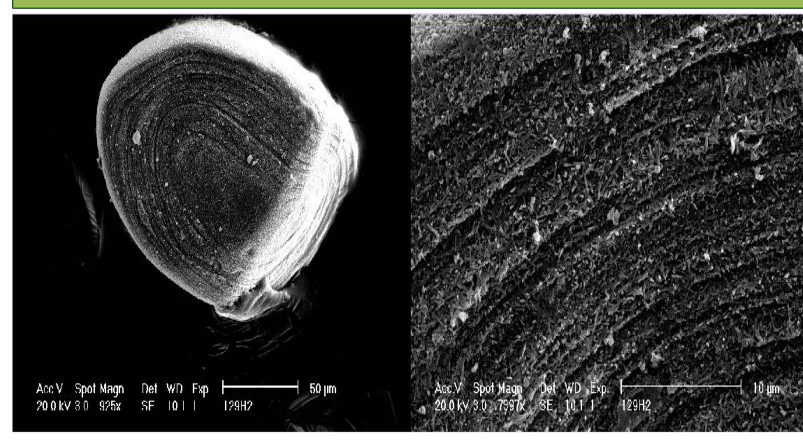

***Figure 4:** A SEM photomicrograph of a nearly whole ooid (left), where the concentric structure around central fecal pellet nucleus visible. Note that concentric layers are clearly visible in defined and distinct positions (right). The sample was lightly etched in dilute hydrochloric acid. Sample from Core 20, 129 cm.*

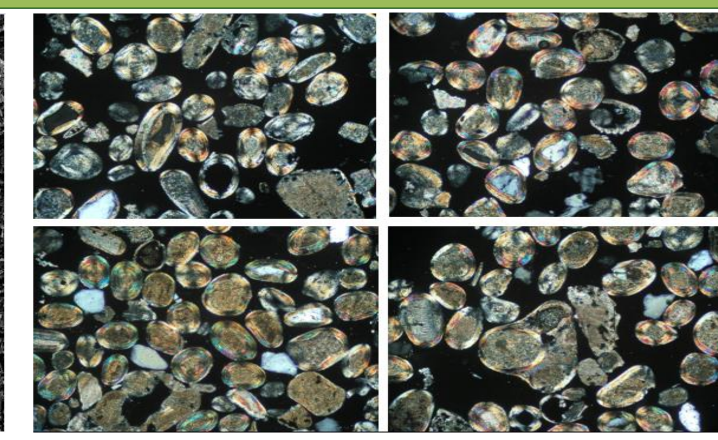

***Figure 5:** Sand-sized components of Core 20 (~220 cm). Most ooid grains are highly polished and between 150 and 250 microns in diameter. Laminated cortex of ooids is generally well preserved. Width of photographs are 1.5 mm.*

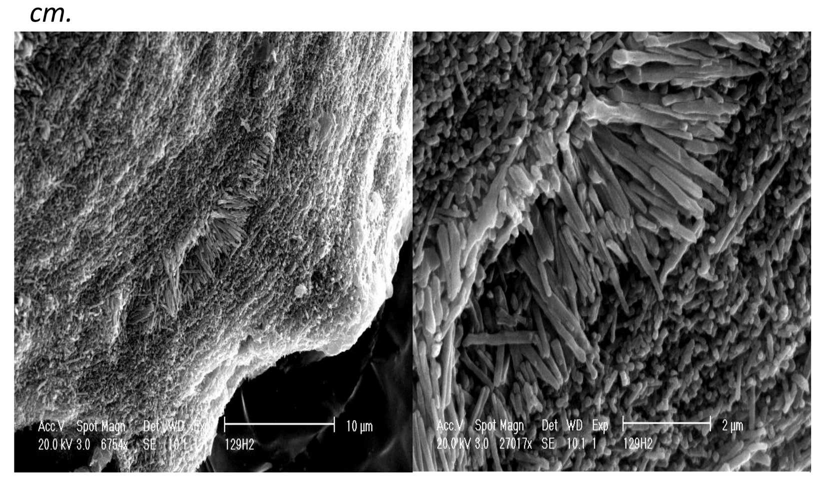

***Figure 6:** Elongate crystals visible within concentric layer of the grain cortex. The crystals are most often oriented perpendicular to the concentric layering. Sample from 129 cm, Core 20.*

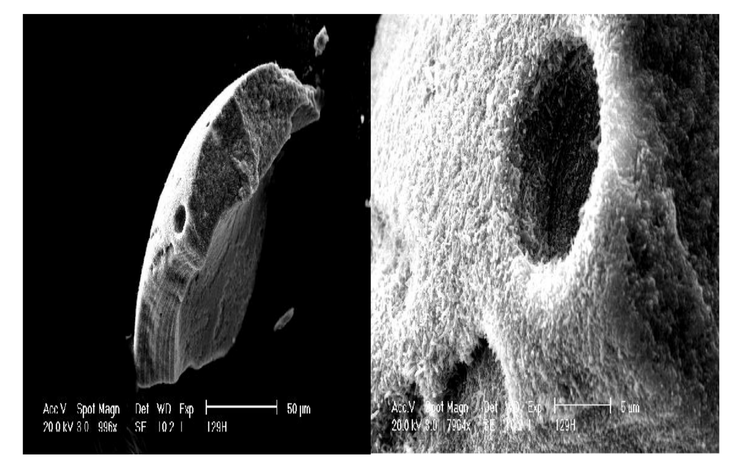

***Figure 7:** Example micro-bore within ooid cortex (left). An enlargement of the boring (right) show surface micritization (recrystallization) with preserved laminae below. Sample is from 129 cm, Core 20.*

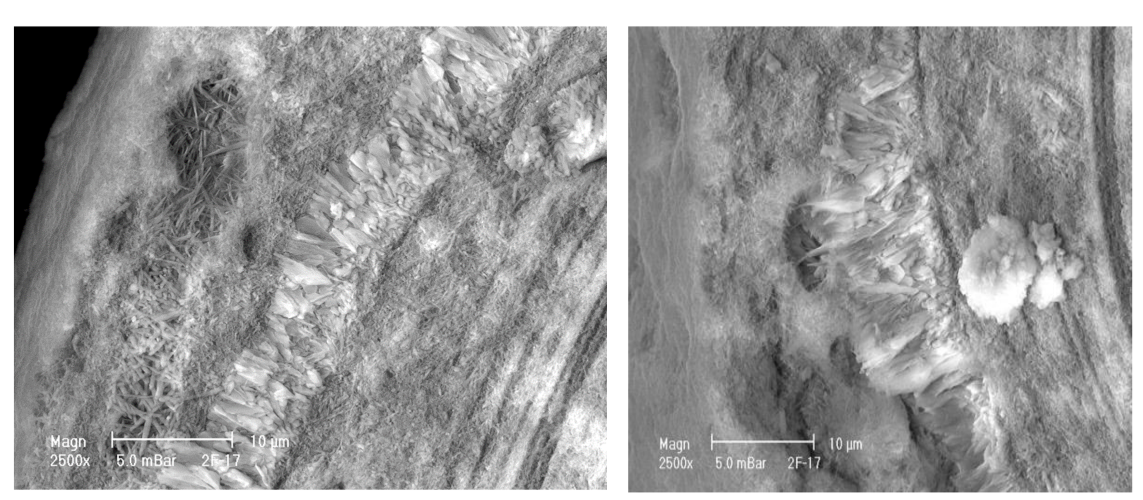

***Figure 8:** Presence of elongate and botryoidal crystals within outermost concentric layers of the ooid cortex. Sample is from Core 2F at a depth in core of 17 cm. Figure is from McNeill, unpublished.*

***Figure 9:** Example micro-borehole within oolitic grains. Left: whole ooid grain from Core 20 (238 cm) that shows few individual boring traces. Right: close-up of microboring structures in ooid grains from Core 20. Concentric layering visible. 129 cm, 238 cm, Core 20.*

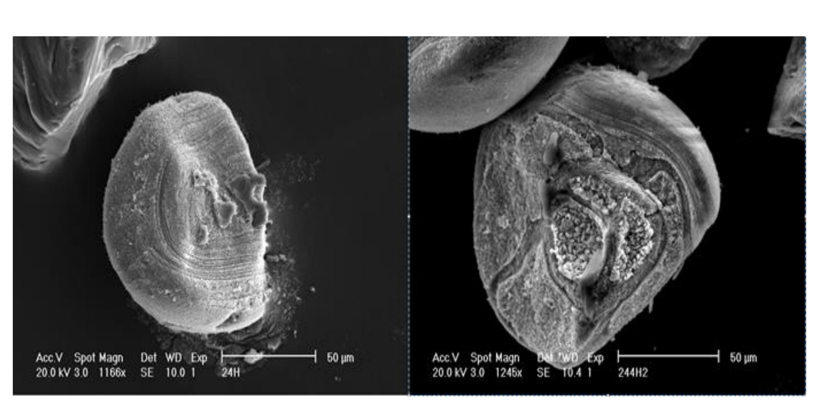

***Figure 10:** SEM and light microscopy confirm the variety of nuclei within the ooid grains. Many contain small mud pellet centers (left), where others have larger detrital (skeletal?) fragments. Note the well-preserved concentric cortex. Sample from 24 cm, Core 20.*

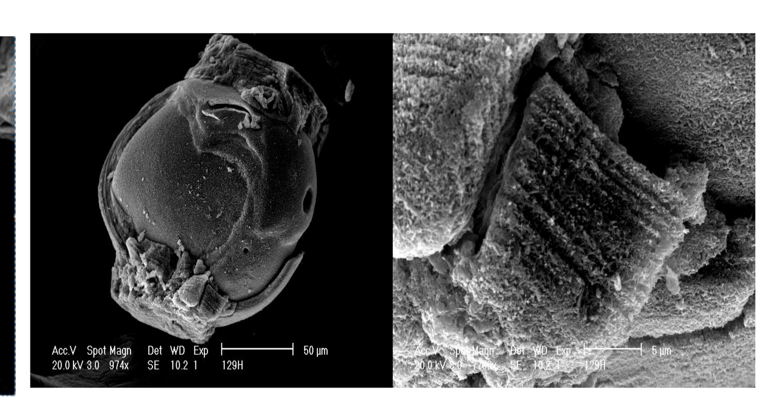

***Figure 11:** Central borehole through ooid grain nucleus (left), and a close-up of the ooid cortex (right) from the lower part of the grain shown at left. Sample is form Core 20, 129cm.*

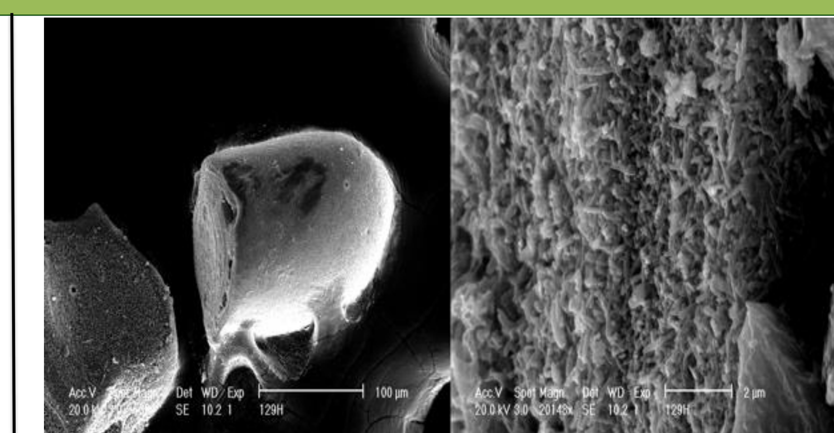

***Figure 12:** Elongate ooid with concentric-laminated cortex that contains several empty irregular voids (left). Close-up of the concentric-laminated cortex with one of the empty voids. Sample is from Core 20 at 129 cm depth.*

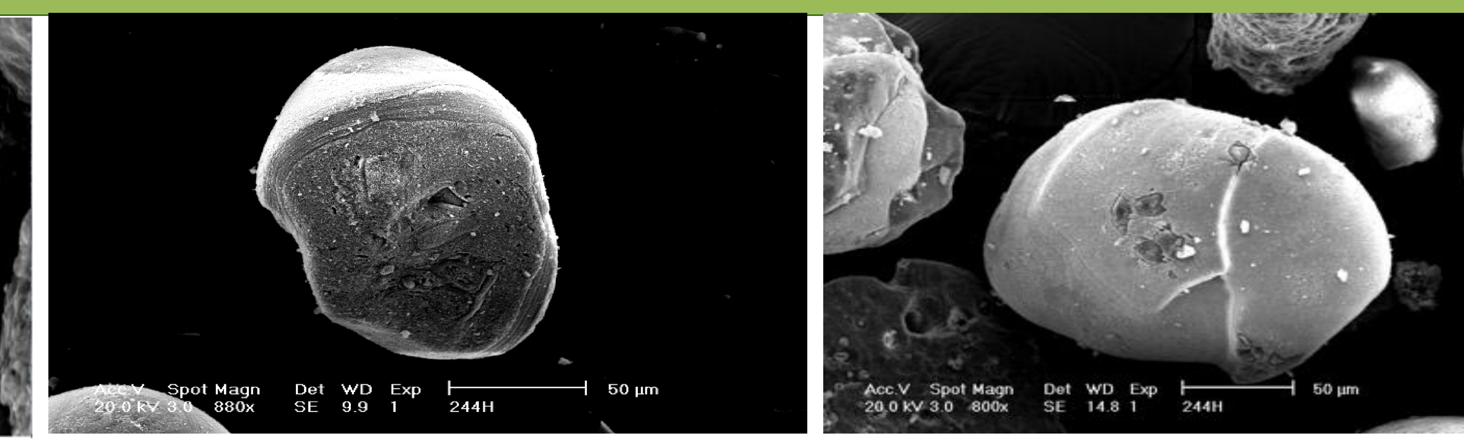

***Figure 13:** Lack of microboring and alteration visible in surface and concentric layers of deeper core ooids, samples from Core 20 at 244 cm depth.*

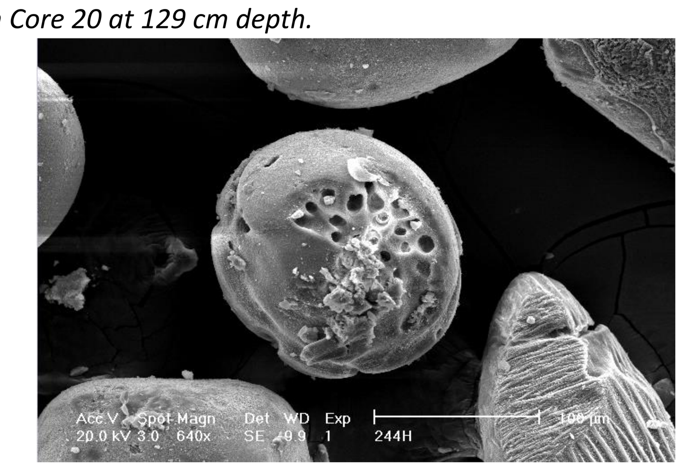

***Figure 14:** Extensive boring present on surface of ooid grain, demonstrates ability of oolitic grains to develop secondary porosity structures along with naturally permeable grainstone structure. Sample from Core 20, 244 cm.*

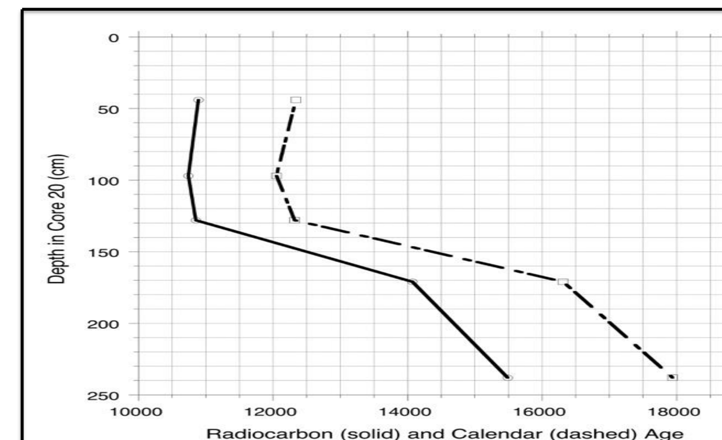

***Figure 15:** Age-depth data for Core 20. Radiocarbon ages are shown as C-14 age (solid line) and as calendar year ages (dashed line).*

***Table 1.** Summary of radiocarbon age dates for NAVO Core 20. These age data were from an unrelated, unpublished study.*

Core 20 Sample No.	Sample Depth in Core (cm)	C-14 age (years BP)	Calendar age (years BP)	Comments
20-44C Beta-207984	44	10,900 +/- 50	12,340	bivalve shell, ooid packstone
20-97C Beta-207985	97	10,750 +/- 60	12,060	bivalve shell, ooid packstone
20-128C Beta-207986	128	10,860 +/- 50	12,320	bivalve shell, ooid packstone
20-171C Beta-207987	171	14,080 +/- 60	16,310	bivalve shell, ooid packstone
238 Beta-181457	238	15,490 +/- 90	17,940	ooid sand, ooid grainstone

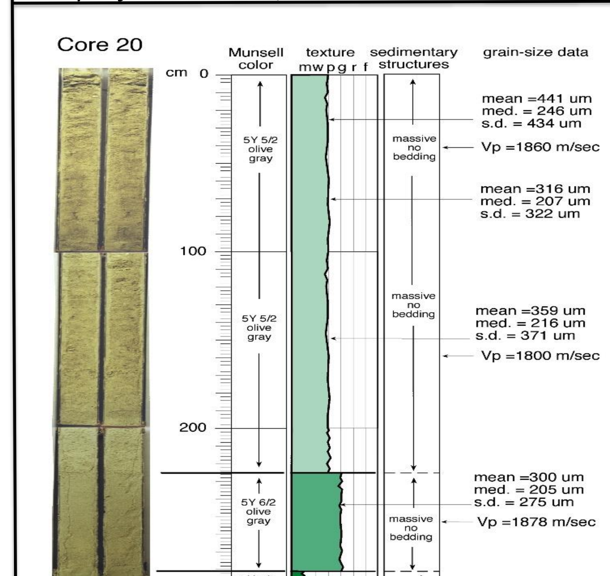

***Figure 16:** Core photograph and core description of Core 20. The textures are mainly grain supported: packstone and grainstone. The grain size and acoustic velocity (from an unrelated study) are shown on the right (figure is from McNeill, unpublished study).*

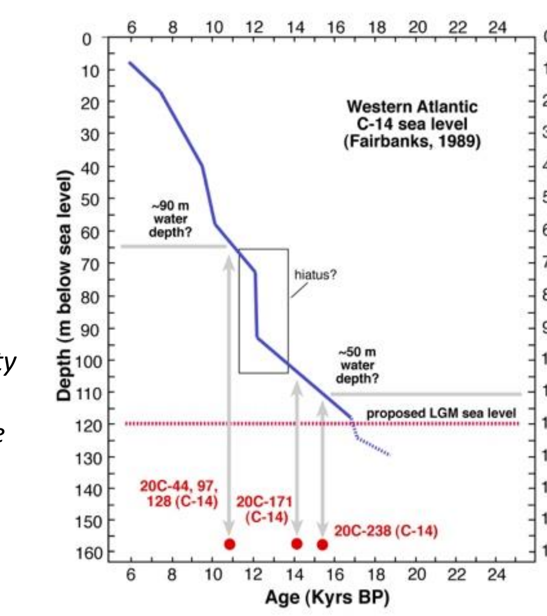

***Table 2:** Core 20 samples used for SEM characterization.*

Depth in core (cm)	Acid Etched Samples or Crushed Samples	Average Grain Size (micron meters)	Samples Taken (200 grains)
24	Both	441	2
40	Both	441	2
69	Acid Etch Only	316	1
129	Acid Etch Only	359	2
236	Both	300	2
244	Both	300	3

***Figure 17:** Simplified sea level curve of Fairbanks (1989) with the proposed last glacial maximum sea level, and the depths of three radiocarbon samples from Core 20 shown in calendar years before present. The depth offset suggests water depths from 50 m to nearly 90 m.*

Discussion

- With reference to radiocarbon ages (Table 1, Figure 15, Figure 17) and the water depths at which the cores were collected (Figure 1), the ooids formed below the last glacial lowstand. [7]
- Ooids below the 3200-year hiatus display differences to those located above the discontinuity: less endolithic boring, a mix of tangential and radial crystal orientation, and less evidence of micritization (Figure 5, 9, 13).
- Typical alterations were small tracks of boring visible on the surface (Figure 9, 14) or larger structures that disrupt concentric layer growth (Figure 7, 9, 11, 12).
- The rate and type of carbonate precipitation (based on tangential or radial crystal orientation) that occurred was variable and may have led to discontinuities in concentric layer formation (Figure 6, 8, 11)

Conclusions

1. Ooids from Core 20 off southeast Florida at a depth over 150 m were produced at depths below the last glacial lowstand (of ~120 m). Core 20 contains a hiatus of ~3200 years at 171 cm depth confirmed by carbon-14 ages. Ooids below the 3200-year hiatus display slight differences: less endolithic boring, a mix of tangential and radial crystal orientation, and a tendency to display less evidence of micritization

2. Tangential as well as radial/botryoidal crystal structures are found within Core 20. Most modern (Bahamas, Turks and Caicos) shallow-water ooids typically do not contain radial structures.

3. Depth of formation, age discontinuity within ooid formation, and unique preservation status, and a lack of intense micritization supports the idea of a deep-water ooid factory.

References

1. Bard et al., 1996 **2.** Di Bella et al., 2019 **3.** Diaz et al., 2014 **4.** Diaz et al., 2017 **5.** Diaz et al 2019 **6.** Dugrid et al., 2010 **7.** Fairbanks 1989 **8.** Flannery et al., 2019 **9.** Gould and Stewart, 1956 **10.** Hanebuth et al., 2008 **11.** Harris et al., 1977 **12.** Harris et al., 2019 **13.** Hine 1977 **14.** Illing, 1954 **15.** Keith and Zuppmann, 1993 **16.** Marino and Santantonio, 2010 **17.** Mariotti et al., 2018 **18.** Milliman et al., 1972 **19.** Roehl et al., 1985 **20.** O'Reilly et al., 2017 **21.** Soloviev et al., 2017 **22.** Trower et al., 2018

Acknowledgments

Dr. Donald McNeill, Dr. Harold Wanless, Dr. James Klaus, Dr. Patricia Blackwelder, The Center for Advanced Microscopy and Center for Carbonate Research (CSL)